X-661-76-132
PREPRINT

ENERGY SPECTRA OF COSMIC RAY NUCLEI: $4<Z<26$ AND $.3<E<2$ GeV/amu

R. C. MAEHL
J. F. ORMES
A. J. FISHER
F. A. HAGEN

JUNE 1976

GODDARD SPACE FLIGHT CENTER
GREENBELT, MARYLAND

Abstract

Energy spectra of cosmic ray nuclei in the charge range $5 \leq Z \leq 26$ have been derived from the response of an acrylic plastic Cerenkov detector. Data were obtained using a balloon borne detector and cover the energy range $320 \leq E \leq 2200$ MeV/amu. Spectra are derived from a formal deconvolution using the method of Lezniak (1975). Relative spectra of different elements are compared by observing charge ratios. Secondary primary ratios are observed to decrease with increasing energy, consistent with the effect previously observed at higher energy. Primary to primary ratios are constant for $6 \leq Z \leq 10$ and $14 \leq Z \leq 26$ but vary for $10 \leq Z \leq 14$. This data is found to be consistent with existing data where comparable and lends strong support to the idea of two separate source populations contributing to the cosmic ray composition.

ENERGY SPECTRA OF COSMIC RAY NUCLEI:

$4 \leq Z \leq 26$ and $.3 \leq E \leq 2$ GeV/amu

I. INTRODUCTION

One of the most important aspects of the chemical composition of the cosmic rays is the variation of that composition with energy. If we are to understand the nature of the cosmic ray source (or sources) and how the cosmic rays propagate through the galaxy we must measure the details of the energy spectra on an element by element basis. In the past several years it has been established that the ratio of cosmic ray secondary (i.e. nuclear spallation products produced in propagation) to primary nuclei (i.e. nuclei found in the cosmic ray source) decreases as a function of energy for very high energies, $T > 10$ GeV/amu (Juliusson, et al, 1972, Smith et al., 1973; Ormes et al., 1973; Webber et al., 1973). In addition, it also appears that the ratios of at least some primary nuclei are energy dependent at such energies (Ormes et al, 1973; Juliusson, 1974, Lund et al, 1975). It has been postulated that the secondary to primary ratio variations may be due to an energy dependent leakage from the galaxy at high energies (Webber et al., 1973, Juliusson, (1974). This phenomenon necessarily results in a somewhat smaller effect in the primary ratios also. However, if we find the energy dependence of the ratios of primaries to be in quantitative disagreement with predictions based on the secondary/primary ratios it becomes necessary to evoke some additional, different phenomenon such as multiplicity of source types (Ramaty et al., 1973) or confinement volumes (Cartwright, 1973).

It is now generally accepted that such energy dependences do exist Lund (1973) has summarized the most current observations. In order to differentiate between source and propagation effects it is important to clarify and quantize the variations in the energy spectra.

Specifically, at the present time we do not know how low in energy these variations occur and it is to this question we address ourselves in this paper.

Using data obtained from a high altitude balloon borne detector, we have determined the differential kinetic energy spectra of various cosmic ray nuclei in the charge range $4 \leq Z \leq 28$. The data are derived from the response of an acrylic plastic Cerenkov counter and cover the kinetic energy range 400 MeV/amu $\leq T \leq$ 2100 MeV/amu. Although this is a reasonably narrow energy range it is a crucial region. It will allow us to understand if and how the variations in energy spectra observed at higher energies extend to lower regions of the energy scale. These data are not the first observations in this energy range but our high statistical accuracy, good charge resolution and rigorous mathematical treatment of the Cerenkov counter response allow some interesting new conclusions.

II. DETECTOR SYSTEM & BALLOON FLIGHT

The data we report on here are from a high altitude balloon flight from Thompson, Canada in August, 1973. The detector system, shown in Fig. 1, has been described in detail elsewhere (Fisher et al., 1973). The details of the balloon flight are given by Hagen (1976).

For this analysis we make use of only the top two scintillators, S1 and S2; the Cerenkov counter and the spark chamber. The remainder of the system, a stack of scintillators below S2 not shown in Figure 1, was intended for use in the isotope mode and the results from that analysis are published elsewhere (Hagen et al., 1975; Fisher et al., 1976). The live time for the flight was 3.14×10^4 sec and the geometric factor for this analysis was 2740 $cm^2 sr$.

Before we can derive energy spectra of individual elements it is necessary to have sufficiently good charge resolution such that the contamination of even the most rare chemical species by more abundant neighboring elements is negligible. The details of how the determination of charge is accomplished are considered elsewhere (Ormes et al., 1975). For our purposes it is sufficient to show the resulting charge histograms. These are shown in Figure 2 for two cases: all of the data and just that subset for which $C/C_{max} \leq 0.8$, where C is the classical Cerenkov response given by

$$C = \overline{K}\, Z^2\, (1-1/\beta^2 n^2). \qquad (1)$$

In this equation $\beta = v/c$, n is the index of refraction of the Cerenkov radiator material (n = 1.49), and $\overline{K}$ is a constant. C_{max} is the value of C for $\beta = 1$. These two histograms clearly indicate the degradation of the charge resolution at high energies, most likely due to the energy dependent Landau fluctuations in the scintillator response. Note even though the delta ray distribution is proportional to Z^2, the net effect is charge dependent as well as energy dependent. This occurs because at high energies some of the delta rays move farther away from the core of the track in the scintillator. Light produced by these particles will exhibit different degrees of saturation from the observed Z dependence of the saturation of the core of the track. This effect can result in a contamination of rare species by more abundant high energy particles of lower charge so it will affect the derivation of the energy spectra of the less abundant species. We will consider this problem in more detail.

In Figure 3 we show the observed response of our Cerenkov counter as a function of β. We find that the actual response observed is a sum of three components; 1) the classical Cerenkov signal as given in

equation (1) above; 2) scintillation in the acrylic plastic; 3) Cerenkov radiating delta rays. The third component is proportional to Z^2 and is distinguishable from the classical Cerenkov signal only through the β dependence of the delta ray distribution. The net effect of the second and third of these contributions is to alter the β dependence of the Cerenkov response from what would be expected if we had only the classical Cerenkov response. Lezniak (1975) has taken this into account by introducing a small perturbation into the index of refraction to account for the additional light from the second two components. We have not taken this approach but instead used an alternative method which we find to be more accurate. Based on measurements of range (from the stack of scintillators below S2) for particles with energies below the Cerenkov threshold we empirically determine the β-dependence of the scintillation in the Cerenkov radiator (Fisher et al., 1976). We then add this to the calculated β-dependence of the delta rays (a relatively small effect) and subtract the sum from the observed Cerenkov pulse height, leaving only the classical Cerenkov response. For particles above the Cerenkov threshold, the β-dependence of this correction is not large and is similar to the β dependence of the plastic scintillators.

The result of this analysis is a series of Cerenkov pulse height histograms, one for each charge, from which we derive the kinetic energy spectra. Fig. 4 shows the carbon spectrum; the fit to the spectrum in this figure will be discussed below. The position of the β=1 peak, when derived by the procedure outlined by Lezniak (1975), scales as Z^2 as predicted by equation (1) to better than 0.2%. Since the distribution is not symmetric about the β=1 point, this result is not obvious from the raw data without accounting for the charge dependence of the resolution.

III. DERIVATION OF THE ENERGY SPECTRA

Since the resolution of the Cerenkov counter is a function of both charge and velocity the uncertainties arising in deriving kinetic energy spectra by simply dividing the data into C/C_{max} pulse height bins are large and difficult to evaluate. Therefore, these uncertainties can cause charge and energy dependent effects which can easily be misconstrued as real energy spectra differences among the elements. Accordingly, the method we us to derive the energy spectra is a formal mathematical deconvolution of the Cerenko pulse height histogram which rigorously accounts for the variations in resolution. As derived by Lezniak (1975), the formulation of the problem is as follows: For a given element the observed Cerenkov pulse height histogram, f(x), is the convolution of the true differential energy spectrum, j(T) with the resolution function $F(X,X'(T'))$ of the detector.

$$f(x) = \int_{T_{min}}^{T_{max}} F(X, X'(T')) \; j(T')dT' \qquad (2)$$

T_{min} corresponds to the Cerenkov threshold and T_{max} is a sufficiently high energy such that $\int_{T_{Max}}^{\infty} j(T')dT' \sim 0$.

Since we know the detector resolution, we can invert equation (2) and solve for j(T). We have done this for the more abundant nuclei and have derived j(T) for each of these elements subject to the constraint that the spectra be smooth (Lezniak, 1975). We find that using this procedure we can fit the observed pulse height distributions quite accurately. The "best fit" reduced χ^2, i.e. the total χ^2 divided by the number of degrees of freedom, is on the order of one or less for every case. As an example, figure 4 shows the carbon pulse height distribution with the results of the best fit deconvolution superimposed upon it. The reduced χ^2 for the fit is $\sim$ 0.9.

The smoothness constraint has very little effect on the major features of the spectra which monotonically decrease with increasing energy. Of course, when this constraint is removed the resultant χ^2 becomes somewhat lower but small local features of low statistical significance may be subsequently superimposed on the spectra.

The analysis depends critically on the resolution of the Cerenkov counter. If either the wrong resolution and/or the incorrect location of the $\beta=1$ point is used the χ^2 becomes large and the fit poor. Fortunately, we know the location of the $\beta=1$ peak quite accurately and are able to predict the resolution as a function of Z from scaling the resolution observed in laboratory calibrations. However, we treat the resolution effectively as a free parameter and allow it to vary to minimize χ^2_R. This is done to provide a consistency check since the best fit resolution should be consistent with the laboratory calibration data. In Figure 5 we show the best fit Cerenkov resolution found by the deconvolution program as a function of Z. The figure shows the resolution increasing as 1/Z as expected from photo-electron statistics up to Z=14. Above that point the resolution effectively becomes independent of charge, indicating that photo-electron statistics are no longer the dominant factor in determining the resolution. This is quantitatively consistent with charge independent uncertainties such as residual map errors and time drift which we expect to find in the data.

Before considering the fits to the data, it is necessary to consider possible sources of error. While the formal statistical errors are in most cases less than a few percent, it is important to consider possible

systematic effects. We have carefully analyzed possible biases due to spark chamber inefficiency, nuclear interactions in the detector and discrimination threshold and find any residual uncertainty after making the appropriate corrections to be small. Additionally, we have considered possible electronic effects, such as analyzer non-linearities and, more importantly, uncertainties in the gain charge factor in the Cerenkov counter pulse height analyzer (we use a two range system for improved dynamic range). This analysis consisted of looking for discrete discontinuities such as may be expected if these factors are incorrect. We found no such discontinuities in the raw pulse height spectra or any indication of discontinuities in the deconvolution procedure (this effect would result in a "kinky" spectrum and/or an unacceptable χ^2).

Another possible experimental uncertainty is due to the atmosphere. The extrapolation of the energy spectra to the top of the atmosphere is quite straightforward; we take the best fit spectrum, calculate the energy loss in overlying atmosphere on a bin by bin basis and use the results to extrapolate the spectra. This is the only reliable procedure since the resolution of the Cerenkov counter does not allow for an accurate identification of the energy of each individual event. The extrapolation of the charge composition we require to generate absolute fluxes is somewhat more complicated. We have written a computer program to model the cosmic ray beam as it propagates down through the atmosphere. This program will be described in detail elsewhere but it effectively treats the atmosphere as a slab, making use of the measured nuclear cross sections for nucleus-nucleus interactions where available (Lindstrom et al, 1975) and semi-empirical estimates where no measurements have been made (Tsao and Silberberg, 1975). While it is difficult to estimate the errors in such a calculation (nominally

the cross sections are accurate to 20%), these errors are not energy dependent since the cross sections for nucleus-nucleus interactions become essentially independent of energy for T > 2.0 GeV/nucleus (Tsao and Silberberg, 1975), and the energies in consideration here are T ≥ 320 MeV/amu for nuclei with A ≥ 7. Therefore, although errors in this calculation may cause uncertainties in the absolute values of charge ratios at the top of the atmosphere (and thereby possibly cause some discrepancies among different experimenters that have treated the atmosphere differently) the effect is very likely not energy dependent.

There is one final possible systematic uncertainty which, in effect, is a fundamental limitation to the amount of information about energy spectra which can be extracted from an acrylic plastic Cerenkov counter. This uncertainty is caused by the saturation of the energy dependence of the Cerenkov counter. Since for T ≥ 2500 MeV/amu the Cerenkov response is effectively independent of energy we have no energy resolution at high energies. Therefore, for a large group of particles on the high energy end of our pulse height distribution it is necessary to assume a high energy asymptotic spectrum in order to account for the distribution of the high energy particles in the pulse height spectrum. Using this assumption we effectively calculate how many particles lie in the region of no energy resolution and then account for their spillover to lower pulse heights which contaminates the data in the region where the Cerenkov response is energy dependent. Given the general shape of the cosmic ray energy spectra, the percentage of events in the region of poor and/or no energy resolution is large (J(>1500 MeV/amu)/J(>300 MeV/amu) ≈ 0.5) and therefore the contamination may be significant. Based on high energy (T> 3.0 GeV/amu) observations we characterize the asymptotic spectrum by a power law for which we assume a

spectral index.

Since we are ultimately interested in determining ratios of charges as a function of energy, let us consider the consequences of this assumption for these ratios. If the high energy spectra of all elements are the same this assumption is of no consequence to our observations. However, as mentioned in the introduction, there is a substantial amount of evidence that indicates the high energy spectra may vary among the elements. Unfortunately, most direct measurements of this effect are in the $T \gtrsim 10$ GeV/amu range. As such they are not directly applicable to our problem since the bulk of the events with $T > 2.0$ GeV/amu lie in the 3-10 GeV/amu range, and the spectral indices measured for $T > 10$ GeV/amu may not be representative of these data. In addition, we cannot measure such possible differences directly, so if we observe an energy dependence of charge ratios in the 0.3-2.0 GeV/amu range we are forced to account for the influence of particles with $T > 3.0$ GeV/amu on these ratios indirectly.

We do this as follows: Consider two extreme cases: 1) the assumption that all the energy variation is between 0.3-2.2 GeV/amu, that is the asymptotic value of the spectral index is independent of charge and; 2) the assumption that all the energy variation is above the region we measure. The first case is not really physically plausable, in addition to which it conflicts with the high energy data, but these are the two extreme assumptions and it is fairly safe to assume that either assumption (2) is true or the real case lies somewhere between the two. Figure 6 illustrates these two extremes and shows schematically the limits on the information that can be obtained from taking the ratio of the deconvolved spectra of two elements having different spectra. Case 1 is represented by circles crosses and Case 2 is represented by the crosses, the points at highest energy are intended only to

imply the two cases are limits. The true value of the ratio in this energy range is somewhere in the band between the two cases. It is important to note that these limits provide the maximum amount of information available from an n = 1.49 Cerenkov counter with finite resolution. The width of the band and the minimum energy for which the two cases are separated are functions of the magnitude of the energy variation and the counter resolution.

IV. THE DATA

In Figure 7 we show the results of the deconvolution for the more abundant nuclei using assumption (1) from above. The ordinate is the absolute flux at the top of the atmosphere. The atmospheric extrapolation was done for each energy bin of each element; hence points are centered on slightly different energies at the top of the atmosphere. The method of accounting for nuclear interactions in the atmosphere is that described in Section III above. The reason we have chosen to base these figures on assumption (1) is simply that these data, taken alone, provide no information as to which of the two assumptions is correct so as a first approximation we assume no spectral differences at any energy. When we take charge ratios based on these figures we find this not be the case, as expected, so we use an iterative process as described below to account for the energy variation. It should be noted that the absolute fluxes shown in Fig 7-9 <u>are based on assumption</u> (1) and therefore are subject to substantial systematic errors.

Before we consider these data let us consider the problems encountered with the rare elements due to the energy dependence of the charge resolution as mentioned above. In the case of the odd-Z elements with $8 \leq Z \leq 14$ the statistics are sufficient to warrant a formal deconvolution calculation. However, if we look back at Figure 2 we see that near the

Cerenkov maximum signal the contamination due to the even-Z elements may be as high as 20% and is certainly energy dependent. Note that the peak to valley ratio between F and O decreases by 50% when all data are included. Fortunately, at lower energies this problem is less severe so we can indirectly infer spectra for F, Na and Al over a narrow energy band as follows. For each of these elements we take the ratio of the number of events in a bin of given Cerenkov pulse height width to the number of events in the same bin of one of the adjoining even-Z elements. We then multiply that number by the flux of the bin of the even-Z nuclei as calculated from the deconvolution program, thereby deriving the spectrum of the odd-Z nuclei. After correcting for the mass dependent difference in interactions in the detector, the odd-Z nuclei are then extrapolated to the top of the atmosphere. In doing this it is absolutely imperative that each odd-Z spectrum be compared to the most nearby even-Z nucleus in order to minimize the charge dependence of the resolution. In Figure 8 we show the results of this analysis.

The elements with $Z > 14$ (excepting iron) present a similar problem. While they are not contaminated by more abundant nuclei, the statistical accuracy in this group is such that the deconvolution calculation becomes somewhat uncertain. We, therefore, use the same method as outlined above tor the odd-Z nuclei to infer spectra in this region. While this may introduce uncertainties due to the Z dependence of the resolution as outlined above, in this region these effects are not severe and not the limiting factor. (See Fig. 5) In Figure 9 we show the spectra of nuclei, grouped in some cases due to statistical limitations, derived in this manner.

If we consider Figures 7-9 we see that in the energy region under consideration none of the spectra can be characterized by a power

law in kinetic energy. This is true also for power laws in total energy or rigidity. While an exponential kinetic energy spectrum seems to fit somewhat better the fit is still not good in any case so we choose not to characterize the spectra by spectral indices.

Note also that we do not see the peak differential flux on any of the spectra but they continue to rise with decreasing energy. This is somewhat surprising since earlier measurements show a maximum in differential flux in the region we observe (Webber, 1973). This difference is most likely attributable to solar effects. Webber's C+O spectrum shows a maximum at about 600 MeV/amu in 1970, the time of solar maximum. Between 1970 and 1971 neutron monitor data shows a sharp increase in counting rate (Lockwood, 1972) and the maximum in Webber's C+O spectrum becomes less sharp and moves down to about 300 MeV/amu. Our observations in August 1973, are at solar minimum hence we expect even smaller solar effects on the spectrum than Webber's 1971 data and this is consistent with our observations. In Table I we show the differential fluxes we derive at 1 GeV/amu in comparison with those of other workers. The agreement is quite good in general, however, our iron flux is about 25% lower than earlier data, probably due to differences in charge grouping effects in this region. Due to resolution differences and uncertainties in the extrapolation through the atmosphere, we feel this discrepancy is due to systematic differences in data analysis procedures. Note that when we quote fluxes of the $25 \leq Z \leq 27$ group the discrepancy is somewhat smaller. This is due

to the fact that our Mn/Fe ratio is ~ 0.2 while most other workers measure Mn/Fe ~ 0.1. We believe that the major source of the disagreement in the iron region is the uncertainty in peak position and shape due to scintillator saturation. Only the data of Benegas et al (1975) is unaffected by this problem and is therefore probably the most reliable with respect to the fine structure of the composition of the iron group. In addition, both the Si and the Fe fluxes of Garcia-Munoz et al (1975a) are somewhat higher than those of other workers, however the Si/Fe ratio is in essential agreement among all the groups. Since in general systematic uncertainties in absolute fluxes are variable among different types of experiments we feel these different sets of data are in reasonable agreement.

V. DISCUSSION OF THE RESULTS

Since the spectra we have derived are not amenable to representation by spectral indices and we are interested in comparing the elements it follows that elemental ratios as a function of energy is an advantageous way to look at the data. In Figure 10 we present a series of such ratios from B to Fe with the lighter element of each pair in the numerator and the heavier element in the denominator. Elements for which we infer the spectra by the ratio method are not included in this figure These ratios have been extrapolated to the top of the atmosphere but no attempt has been made to account for solar modulation since data were taken at solar minimum and, in addition, are at high enough energy that the major effect of transport through the solar cavity is the loss of about 200 MeV/amu for each nucleus. A/Z dependent effects are probably small so the effect of solar modulation on these ratios is not likely to be severe.

In Figure 10 for the cases where the ratios are energy dependent we show the two assumptions discussed above, the dots representing the case where all the energy variation is between 0.3-2.0 GeV/amu and the crosses representing the case where all the variation is assumed to be

at T > 2.0 GeV/amu. One way which we can characterize the second case is by introducing the concept of an "effective $\Delta\gamma$". If we make the assumption that all of the observed variations are due to spectral differences at higher energies, we can derive what these differences must be. In Table II we show the "effective $\Delta\gamma$'s" so derived. This table will be discussed further below.

Superimposed on Figure 10 are the results of a propagation calculation assuming an exponential path length model with a leakage length of 5 gm/cm^2 (we assume 90% H and 10% He for the interstellar gas). In this calculation we assume that the source composition is independent of energy so variations in the results are caused by the energy dependence of the nuclear interaction cross sections. The calculation is described in detail elsewhere (Hagen, 1976), the cross sections we use are from the semi-empirical formula of Silberberg and Tsao (1973a, 1973b).

Recall that, of the elements included in Figure 10, boron is the only one which is exclusively secondary and as expected we see B/C dropping somewhat toward higher energies. Be is excluded from this analysis since there is evidence that some small but possible significant fraction of the Be with T > 2.0 GeV/amu was unable to fire the system in the coincidence mode we require for this analysis.

The C/N ratio is essentially constant but rises by about 6% over the energy range we measure here. This effect is in good agreement with what is expected from propagation due to the energy dependence of the cross sections. N/O is similar, very nearly constant, implying the C/O ratio is essentially independent of energy, varying by less than 6% between 400 MeV/amu and 2100 MeV/amu. The O/Ne ratio

appears flat with the exception of the highest energy point. This point falls above the others by about two sigma and does not seem to be associated with any smooth variation in energy. The Ne/Mg ratio, on the other hand, is the first in this series that show a clear trend to vary systematically with energy in a way which is clearly not statistical. The Mg/Si ratio continues this trend, implying the Si spectrum flattens considerably above 1.0 GeV/n with respect to Ne or O. However, when we continue this procedure to the Si/Fe ratio we find that the energy dependence disappears, implying Si and Fe have essentially the same spectra. The variation of less than 5% between 500 MeV/amu and 2100 MeV/amu that we observe in the Si/Fe ratio agrees with the variation predicted by the energy dependence of the cross sections used in the propagation without introducing an energy dependent pathlength. The last ratio shown in Figure 10 is O/Fe which, obviously, is energy dependent, the variation being on the order of 25% over the energy range.

The remarkable feature of Figure 10 is that the significant energy variation occurs in the $10 \leq Z \leq 14$ group with those elements having $Z \leq 10$ being similar and Si and Fe similar. This is apparently an unexpected result. However, if we compare our data with other workers we see that where there exists comparable data, there is general agreement. In Figure 11 we show the B/C ratio from our data compared to other workers. This is plotted as a (Be+B)/C ratio since the data of most other workers is given in this form. Since our Be measurements are not reliable at high energy we have used our Be fluxes at $\sim$ 500 MeV/amu and the assumption that the Be/B ratio is independent of energy to normalize our B/C ratio to the (Be+B)/C ratio of the other workers.

In Figure 11 we also show the Si/C ratio and the Si/Fe ratio. Figure 12 shows the Fe secondary/Fe ratio. We see from Figures 11 and 12 that there is, in general, good agreement among the various experimenters on the energy dependence of these ratios. There are some systematic differences in the absolute values of the ratios, specifically for Si/Fe. This ratio has values from the various groups varying by $\pm 15\%$ around the mean of 1.5, but as is the case with the absolute fluxes we feel this variation is understandable in terms of possible systematic differences among / analysis techniques employed for the various sets of data. Figure 11 indicates the Si/Fe ratio can be understood in terms of energy independent leakage propagation with an energy independent source ratio.

Figure 12 indicates the same thing for the $21 \leq Z \leq 24/Z = 26$ ratio. This is to be expected since 21 Z 24 are believed to be almost exclusively iron secondaries. The absolute values of the ratios of primary nuclei from the propagation calculation agree with observation due to the fact that the source composition was chosen to fit the data, however the secondary/primary ratio and the fact that this ratio is energy dependent in a manner consistent with the energy dependence of the cross sections used in the propagation calculation provides a degree of confidence in the results of the calculation.

In Table III we present our data in comparison to the recent satellite measurements of Julliot et al (1975). The two sets of data are not directly comparable since the data of Julliot et al (1975) are integral data taken as a function of cutoff rigidity variation along the orbital path of the ESRO T-1 satellite and the different bins represent different cutoff rigidities. $\overline{T}$ is the most probable energy therefore we compare our data at $\overline{T}$ but their integral measurements have a tendency to smooth out possible variations. Note

that the higher Fe/O ratio they measure is quite natural since their data is based on rigidity cutoff and $A/Z|Fe > A/Z|O$. At around 5.0 GV assuming ^{56}Fe) we expect the Fe/O ratio to be about 20% higher for a rigidity cutoff measurement than for a direct differential kinetic energy measurement and in Table III we show this correction to our data. Note that the effect on the C/O ratio is $\leq$ 1% since C and O are predominantly A/Z = 2.0 nuclei (Fisher et al, 1976). The difference between rigidity and energy cuts will also be present in the Be+B+N/C+O ratio since ^{7}Be, ^{9}Be, ^{10}Be, ^{11}B and ^{15}N all have A/Z 2.0. The precise magnitude of the effect depends on the isotopic composition in a more complicated way than the Fe/O ratio. The result, as shown in the table, is about 7% increase in the ratio.

Figure 11 clearly indicates the variation in the Be+B/C and Si/C ratios are not consistent with an energy independent source ratio with energy independent leakage length. In the case of Be+B/C, since Be and B are secondaries we can attribute the energy dependence to an inverse energy dependent of the leakage length as proposed by Juliusson (1973). However, in the case of Si/C where neither element has a substantial secondary component, we are forced to conclude that this energy variation is a fundamental property of the source. Before we can understand this property we need to consider the energy variations in the ratios of elements between C and Si. Unfortunately, while the above comparisons show that our data agree favorably with those of other workers, the most significant observation in the current data is the energy variation in the $10 \leq Z \leq 14$ group and there exists no data to which this can be directly compared. However, if we compare the "effective $\Delta\gamma$'s" with direct measurements at high energies, also shown in Table II, we find no inconsistencies. This comparison obviously cannot be made directly since our "effective $\Delta\gamma$'s" by definition are most

influenced by the region $2.0 \leqslant T \leqslant 10$ GeV/amu and the data of Ormes and Balasubrahmanyan (1973) are relevant to the range 3 to 30 GeV/amu while the measurements of Juliusson (1974) are for higher energies ($T > 20$ GeV/amu). However, Table II does allow for qualitative comparison of trends in spectral indices and shows no inconsistencies.

VI. CONCLUSIONS

As stated in the introduction it is possible that energy dependent charge ratios may be caused by propagation effects and/or sources differences. While the L/M ratio energy variations might be a similar propagation effect to the one seen at high energy, it is extremely difficult to see how the type of variation we observe among the constituents of the primary group could be anything other than an indication of a multiplicity of sources. It has been suggested by Ramaty et al. (1973), based on high energy iron spectral data, that there are two sources. These data support that hypothesis provided at least a large portion of the Si is identified with the Fe source.

It is interesting to note that variations in both the Fe/O and C/O ratios have been observed by the previously mentioned experiments at high energy but in these data we observe the Fe/O ratio varying but <u>not</u> the C/O ratio. One interpretation of this effect would be that the Fe/O ratio varies down to much lower energy than the C/O ratio. If the Fe/O ratio varies above about 5 GeV/amu but the C/O ratio does not begin to vary until $T \geqslant 20.0$ GeV/amu, the spectral shapes are such that we would observe this effect in the Fe/O ratio but not in the C/O ratio. We therefore conclude that the lower energy limits and magnitudes of these variations are very important points for future study. The physical mechanism

responsible for the variation of the Fe/O ratio could conceivably be quite different from that which causes the C/O energy dependence. For example the Fe/O variation may be a source effect and the C/O variation a propagation effect.

Since we see the primary elements up to Ne having the same spectra and the primary elements with $Z \geq 14$ having the same spectra with Mg about half way between it is informative to consider the Mg data in somewhat more detail. It is obviously impossible for all Mg to have the same source spectrum as the heavier elements since then the primary Mg and the secondary Mg would then have the same spectra and we would observe no variation on the Mg/Si ratio. On the other hand it is conceivable that the Mg at the source has the same spectrum as the lighter elements and the flattening we observe is due to the addition of spallation products from above which have a flatter spectrum. However, from our propagation model we find that only 12% of the Mg is secondary and that is quantitatively insufficient to explain the variation in the O/Mg ratio if the O and Mg source spectra are the same. If this is true it follows that Mg may be found in both sources.

If there are two sources it is possible that the silicon-iron source is local (Rasmussen and Peters,1975). If this is the case several very interesting possibilities arise. First of all there is the obvious possibility of very high energy anisotropies, especially for $Z \geq 14$. Since these elements are very rare, it is probably not possible to look for such an effect with ground based arrays but rather the anisotropies must be detected in the primaries themselves where the charge can be measured directly. This is obviously a difficult experiment requiring large area and long exposure time.

Another possible implication of this model is for measurements of the cosmic ray age. It may well be that if the iron comes from a different,

perhaps local, source that the particles from that source may be of a different, younger age. This might be reflected in the abundance of the isotope $^{26}A\ell$ with a 1/2 life of (7.4×10^5 years). However, a direct measurement of the $^{26}A\ell$ age is also a very difficult experimental task (Fisher et al, 1976). possible radio-active clocks, such as $^{36}C\ell$, are even more difficult to measure directly. Perhaps the most significant aspect of this model is its implications for measurement of cosmic ray lifetime by means of ^{10}Be. At present there is some disagreement as to the amount of ^{10}Be observed (Hagen et al., 1975; Garcia-Munoz et al., 1975b), however it is clear that/a substantial fraction has decayed. Our propagation calculation shows that 20% of the Be produced is ultimately due to elements having $Z \geq 14$. While the propagation calculation obviously must be revised in the case of a two component model, the amount of Fe which undergoes spallation cannot be very different than we now believe since the VH secondary to iron ratio must be preserved. Therefore, if the source of the cosmic rays with $Z \geq 14$ has a different age than the source of the lighter elements the age determination based on ^{10}Be alone becomes somewhat ambiguous. This is a very significant effect if the lighter element component is much older than the heavy element component as presumably would be the case.

If this model is correct, then in order to determine the age of the lighter, $Z < 14$, elements from ^{10}Be it is necessary to determine the age of the heavier elements first from $^{26}A\ell$ or some other radio-isotope. This age would then be indicative of the age of 20% of the Be and the age of the lighter element souce could then be calculated.

To summarize let us reiterate the fact that a detailed knowledge of the charge dependence of the energy spectra of the cosmic rays is

absolutely essential to the understanding of cosmic ray propagation and sources. The previous high energy data based on the relative decrease of the number of spallation products at high energies is probably due to energy dependent escape effects. Our data in the case of boron seems to show that these effects continue down to lower energies, consistent with the propagation hypothesis. However, the energy dependence of the ratios of primary cosmic rays is quite a different problem. Even the high energy data is difficult to explain in terms of propagation and, especially in light of the lower energy data reported here, presents a rather strong case for a source effect. Possible source effects are quite numerous; Z dependent acceleration effects, acceleration of material from different regions in the source or from the ambient interstellar gas, or two or more distinct, physically different types of sources are all possibilities. The energy variations we observe only in the $10 \leq Z \leq 14$ region are difficult to reconcile with charge dependent acceleration effects since the changes occur rapidly over a narrow range of Z. Instead the data seem to indicate more than one source. They do not, of course, allow us to differentiate more than one source region in a given object from more than one type of source object and further observations on this problem are clearly necessary.

Acknowledgements

We wish to thank Dr. J. A. Lezniak for fruitful discussions on the subject of the derivation of the spectra and for supplying the computer program which we used in the deconvolution calculations.

References

Benegas, J. C., Israel, M. H., Klarmann, J., and Maehl, R. C. 1975, Proc. 14th International Conference on Cosmic Rays, Munich, 1, 251.

Cartwright, B. G. 1973, Astrophys. Lett., 14, 157.

Fisher, A. J., Hagen, F. A., Maehl, R. C., Ormes, J. F., and Arens, J. F. 1976, Ap. J., in press.

Fisher, A. J., Ormes, J. F., and Hagen, F. A. 1973, Proc. 13th International Conference on Cosmic Rays, Denver, 4, 2895.

Garcia-Munoz, M., Juliusson, E., Mason, G. M., Meyer, P., and Simpson, J. A. 1975a, Ap. J., 197, 489.

Garcia-Munoz, M., Mason, G. M., and Simpson, J. A., 1975b, Ap. J. (Let), 201, L141.

Hagen, F. A., Fisher, A. J., and Ormes, J. F., 1976, to be published, and Hagan, Ph.D Thesis, U. of Maryland 1975.

Julliot, C., Koch, L., and Petron, N. 1975, Proc. 14th International Conference on Cosmic Rays, Munich, 12, 4118.

Juliusson, E. and Meyer, P., and Muller, O. 1972, Phys. Rev. Lett., 29, 445.

Juliusson, E. 1974, Ap. J., 191, 331.

Juliusson, E. and Meyer, P. 1975, Proc. 14th International Conference on Cosmic Rays, Munich, 1, 256.

Lezniak, J. A. 1975, NIM, 126, 129.

Lezniak, J. A., Kish, J., Preszler, A., and Webber, W. R. 1975, Proc. 14th International Conference on Cosmic Rays, Munich, 1, 283.

Lindstrom, P. J., Greiner, D. E., Heckman, H. H., Cork, B., and Bieser, F. S. 1975, Preprint, LBL-3650.

Lockwood, J. A. 1972, Private Communication.

Lund, N. 1975, Proc. 14th International Conference on Cosmic Rays, Munich, 11, 3746.

Lund, N., Rasmussen, I. L., and Peters, B. 1975, Proc. 14th International Conference on Cosmic Rays, Munich, 1, 263.

Lund, N., Rasmussen, I. L., Peters, B., and Westergaard, N. J. 1975, Proc. 14th International Conference on Cosmic Rays, Munich, 1, 257.

Maehl, R. C., Hagen, F. A., Fisher, A. J., Ormes, J. F., and Simon, M. 1975, Proc. 14th International Conference on Cosmic Rays, Munich, 1, 367.

O'Dell, F. W., Shapiro, M. M., Silberberg, R., and Tsao, C. H. 1975, Proc. 14th International Conference on Cosmic Rays, Munich, 1, 244.

Ormes, J. F. and Balasubrahmanyan, 1973, Nature Phys. Sci. 241, 95.

Ormes, J. F., Fisher, A. J., Hagen, F. A., Maehl, R. C., and Arens, J. F. 1975, Proc. 14th International Conference on Cosmic Rays, Munich, 1, 245.

Orth, C. D., Buffington, A., and Smoot, G. F. 1975, Proc. 14th International Conference on Cosmic Rays, Munich, 1, 280.

Ramaty,, R., Balasubrahmanyan, V. K., and Ormes, J. F., 1973, Science 180, 731.

Rasmussen, I. L. and Peters, B. 1975, Proc. 14th International Conference on Cosmic Rays, Munich 12, 4102.

Silberberg, R. and Tsao, C. H. 1973a, Ap. J., 25, 315.

Silberberg, R. and Tsao, C. H. 1973b, Ap. J., 25, 335.

Smith, L. H., Buffington, A., Smoot, G. F., Alvarez, L. W., and Wahlig, M. A. 1973, Ap. J., 180, 987.

Tsao, C. H. and Silberberg, R. 1975, Proc. 14th International Conference on Cosmic Rays, Munich, 2, 516.

Webber, W. R., Lezniak, J. A., and Kish, J. 1973, Proc. 13th International Conference on Cosmic Rays, Denver, 1, 248.

Webber, W. R., Lezniak, J. A., Kish, J. C., and Damle, S. V. 1973, Nature, 241, 97.

TABLE I

Differential Fluxes at 1.0GeV/AMU* $(m^2\ ster\ sec\ MeV/AMU)^{-1}$

ELEMENT	THESE DATA	UNH[a]	WU[b]	CHICAGO[c]
B	8.40×10^{-4}			
C	2.68×10^{-3}			
N	8.05×10^{-4}			
C+O	5.33×10^{-3}	5×10^{-3}		
O	2.65×10^{-3}			
Ne	4.20×10^{-4}			
Mg	4.70×10^{-4}			
Ne+Mg+Si	1.21×10^{-3}	1.25×10^{-3}		
Si	3.25×10^{-4}		3.5×10^{-4}	4.4×10^{-4}
Fe	1.85×10^{-4}	2.7×10^{-4}	2.5×10^{-4}	3.1×10^{-4}
$25\leq Z\leq27$	2.25×10^{-4}		2.75×10^{-4}	

* Uncertainties as shown in Fig. 7

[a] Webber et al., 1973

[b] Benegas et al., 1975

[c] Garcia-Munoz et al., 1975a

TABLE II

High Energy Spectral Differences

ELEMENT	EFF $\Delta\gamma$ THESE DATA	Observed $\Delta\gamma$'s JULIUSSON (1974) T(>20 GeV/amu)	ORMES et al. (1973) T(>2 GeV/amu)
B	-0.34	-0.2	
B+N			-0.2
C	0	-0.3	
N	0	-0.5	
C+O			*
O	*	*	
Ne	0	-0.3	
10 - 14			+0.1
Mg	+0.10	+0.1	
Si	+0.25	+0.4	
Fe	+0.25	+0.4	+0.6

*Normalization

TABLE III

ENERGY DEPENDENCE OF CHARGE RATIOS

Cutoff Interval (GV)	0 - 2.5	2.5 - 4.0	2.5 - 6.0	4.0 - 8.0	>6.0	>8.0
$\bar{T}$ (GeV/AMU)	0.7	1.2	1.5	2.1	4.7	6.0
Be+B+N/C+O						
Juliott et al. (1975)		0.34 ±0.04		0.337±0.04		0.28 ±0.04
These Data ($\bar{T}$)+		0.32 ±0.02		0.29 ±0.02		
These Data*+						
C/O						
Juliott et al. (1975)		1.01 ±0.07		1.04 ±0.08		1.07 ±0.08
These Data ($\bar{T}$)		1.02 ±0.010		0.98 ±0.01		
These Data*						
Fe/O						
Juliott et al. (1975)	0.116±0.007		0.123±0.007		0.148±0.017	
These Data ($\bar{T}$)	0.081±0.003		0.101±0.003			
These Data*	0.098±0.003		0.122±0.003			

*Normalized to Rigidity Cutoff (see text)

+Be normalized to B as described in the text

NOTE: The data used in this comparison are from Fig. 7

Figure Cpations

Fig. 1

The detector system. The geometry for the coincidence mode considered in these data is given by S1 and S2 coincidence, we discriminate against events with $Z \leq 3$.

Fig. 2

Charge histogram plotted on a semi-logarithmic scale for two cases: all data and only those events with $C/C_{max} \leq 0.8$ (See text).

Fig. 3

Empirical Cerenkov counter response superimposed on the three components of the Cerenkov pulse height as a function of β.

Fig. 4

The Cerenkov pulse height spectrum for Carbon with the deconvolution fit superimposed on it (See text).

Fig. 5

The "best fit" resolution used in the Cerenkov counter deconvolution. The solid line indicates the 1/Z dependence of the fit through the muon calibration point and the dotted line is the same fit with the addition of a 3% error due to all non-photo-electron uncertainties. Note that Be is included in this figure but not in the final analysis. (See text)

Fig. 6

The schematic interpretation of the variation with energy of a charge ratio based on measurements with an acrylic plastic Cerenkov counter.

Fig. 7

Results of the deconvolution calculation extrapolated to the top of the atmosphere for the more abundant nuclei.

Fig. 8

Energy spectra for F, Na, and Al inferred from the data of Fig. 7.

Fig. 9

Energy spectra for elements with $15 \leq Z \leq 24$ inferred from the data of Fig. 7.

Fig. 10

Energy dependence of charge ratios for $5 \leq Z \leq 26$. The solid dots in the figure are for the case where the high energy spectral indices are assumed to be independent of charge and the crosses are for the "effective $\Delta\gamma$'s" given in Table II.

Fig. 11

These data compared to the results of other workers, the sumbols are interpreted as follows. Be+B/C; Δ (Chicago), Juliusson and Meyer, (1975), / / (NRL), O'Dell et al (1975); ∇ (Copenhagen), Lund et al, (1975), O (Berkeley), Orth et al, (1975). Si/C; Δ (Chicago), Juliusson and Meyer (1975); ∇ (Copenhagen), Lund et al, (1975); O (Berkeley), Orth et al, (1975); (New Hampshire), Lezniak et al, (1975). Si/Fe; (Chicago), Garcia-Munoz et al, (1975a); Δ (St. Louis), Benegas et al, (1975); O (New Hampshire), Webber et al, (1973); ∇ (Copenhagen), Lund et al, (1975). The solid line is the prediction of the propagation calculation based on a constant source ratio.

Fig. 12

These data compared to the results of other workers, the symbols are interpreted as follows; Δ (St. Louis), Benegas et al, (1975); O (New Hampshire), Webber et al, (1973). The solid line is the prediction of the propagation calculation assuming the $21 \leq Z \leq 25$ group is absent at the source.

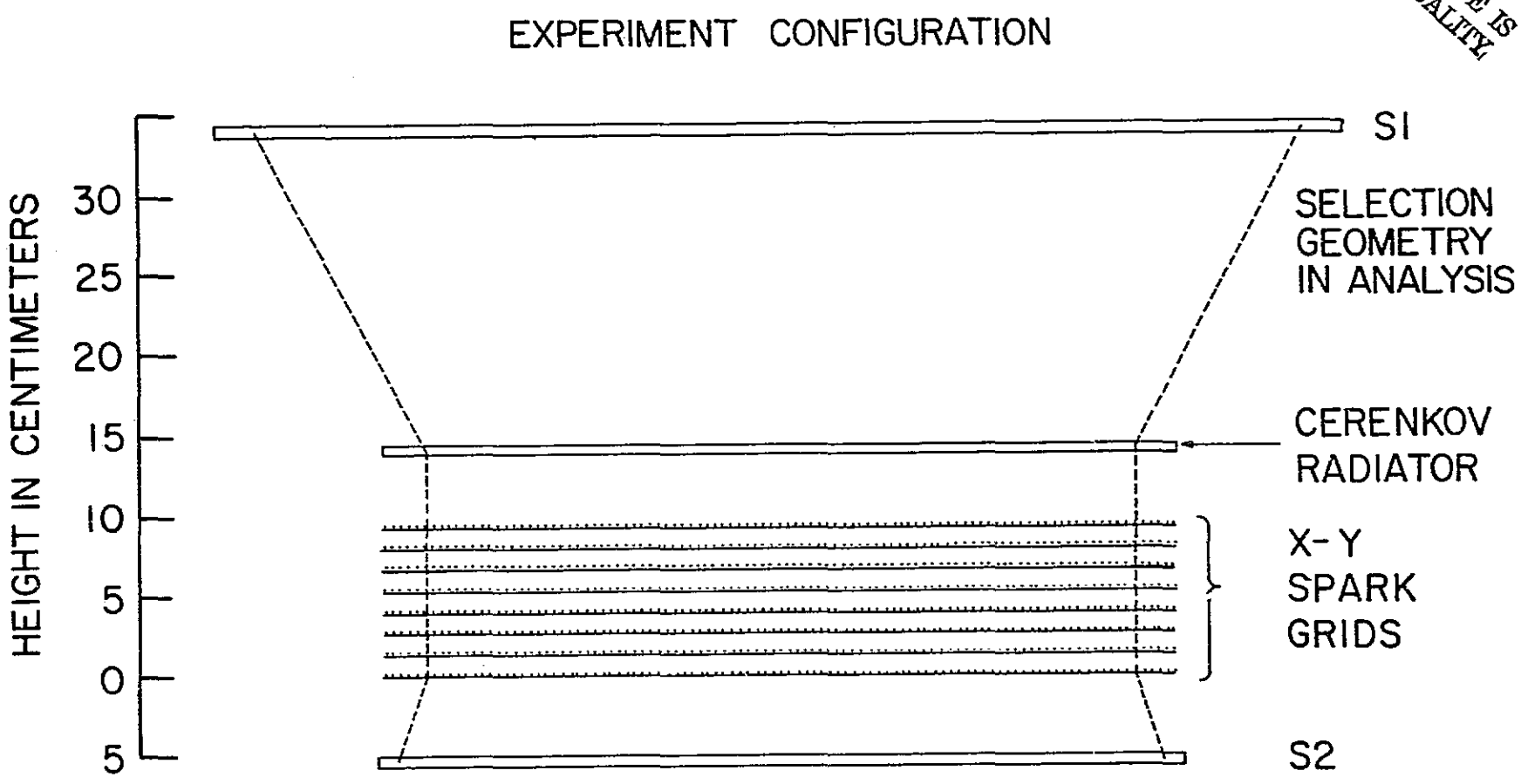

Fig. 1

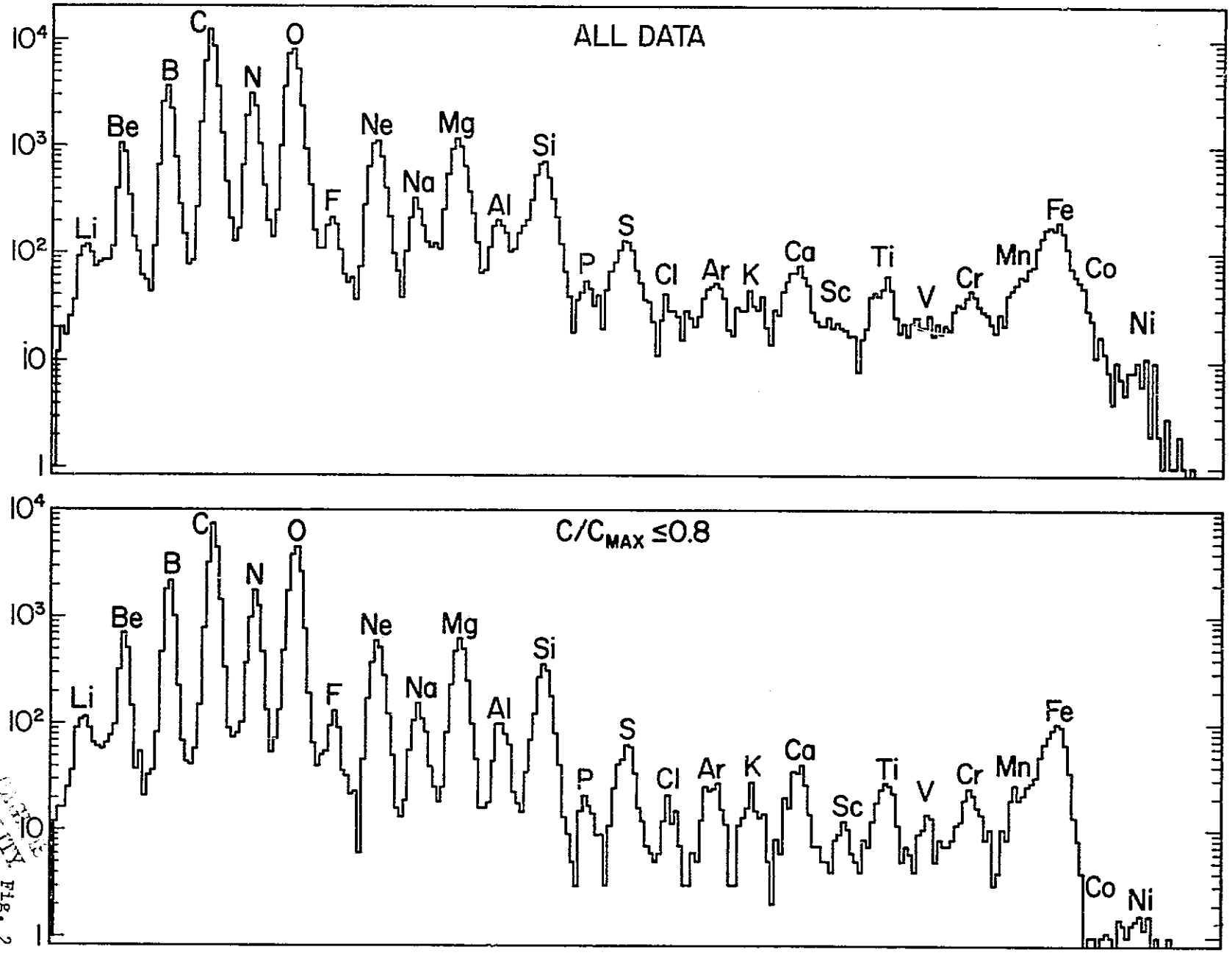

Fig. 2

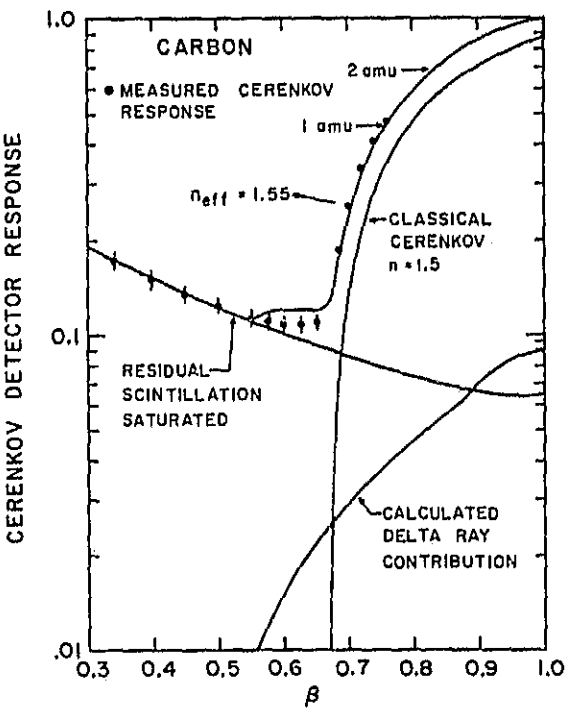

Fig. 3

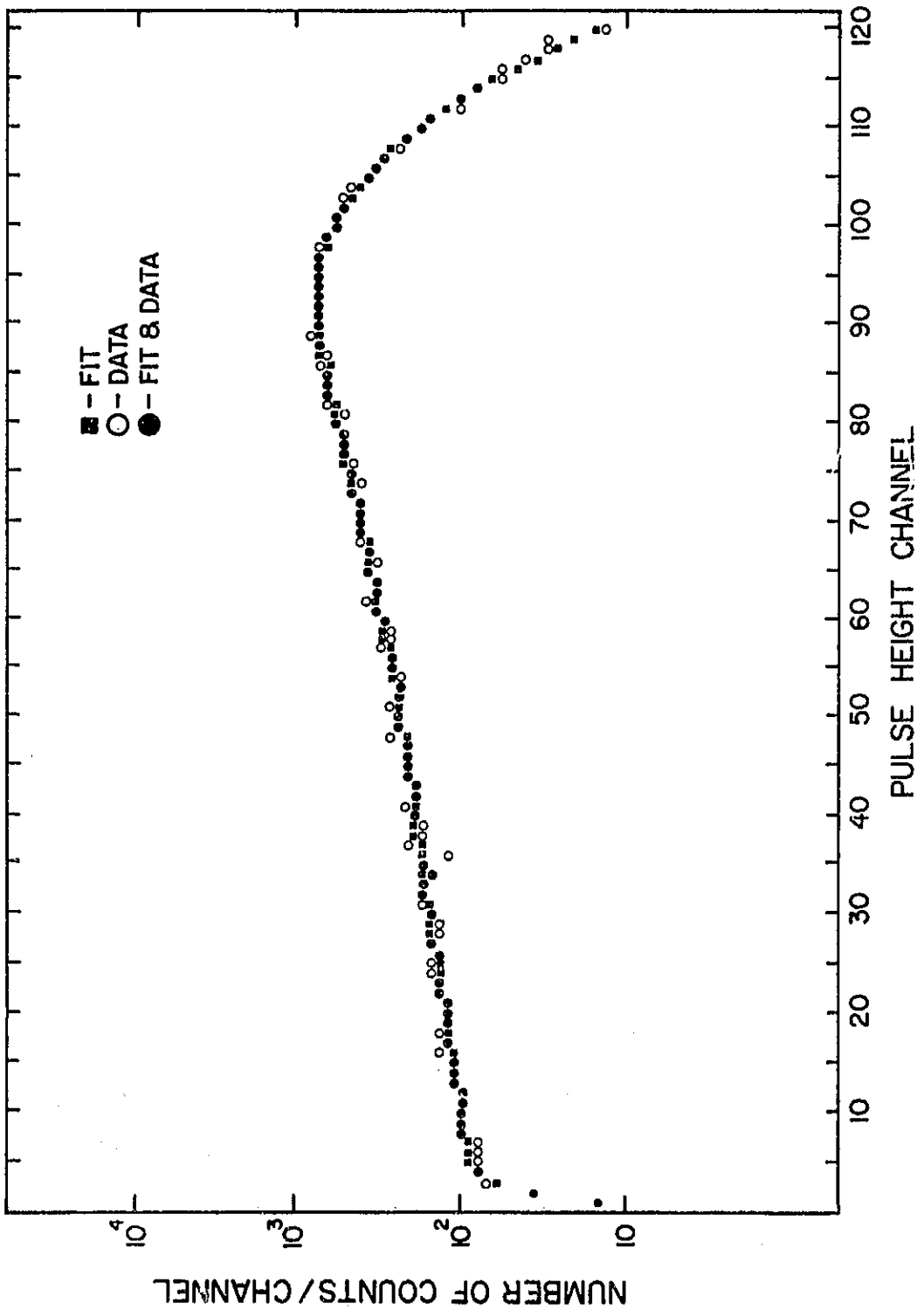
■ – FIT
○ – DATA
● – FIT & DATA
NUMBER OF COUNTS / CHANNEL
PULSE HEIGHT CHANNEL
10
2
10
3
10
4
10
10
20
30
40
50
60
70
80
90
100
110
120

Fig. 4

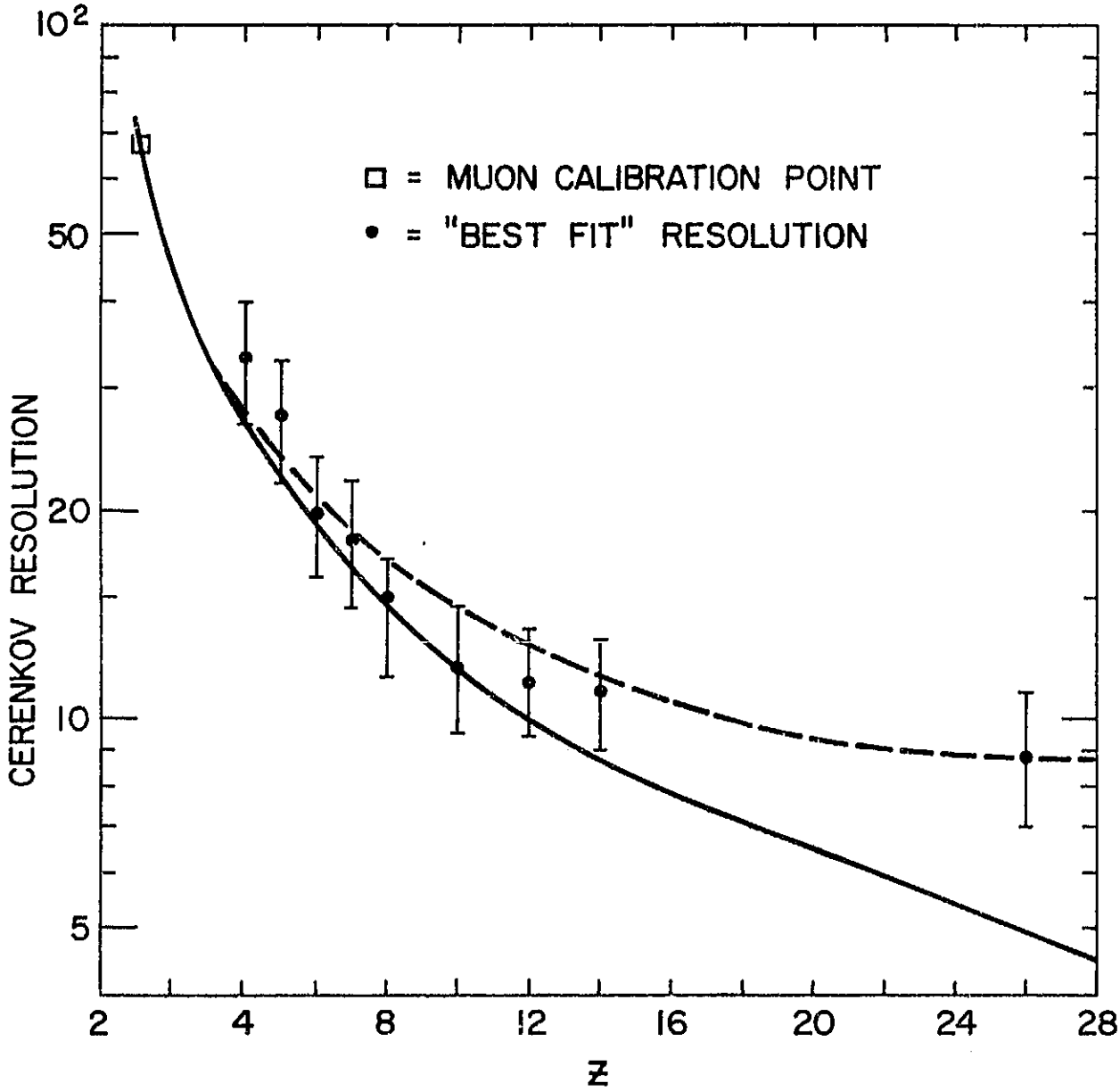

Fig. 5

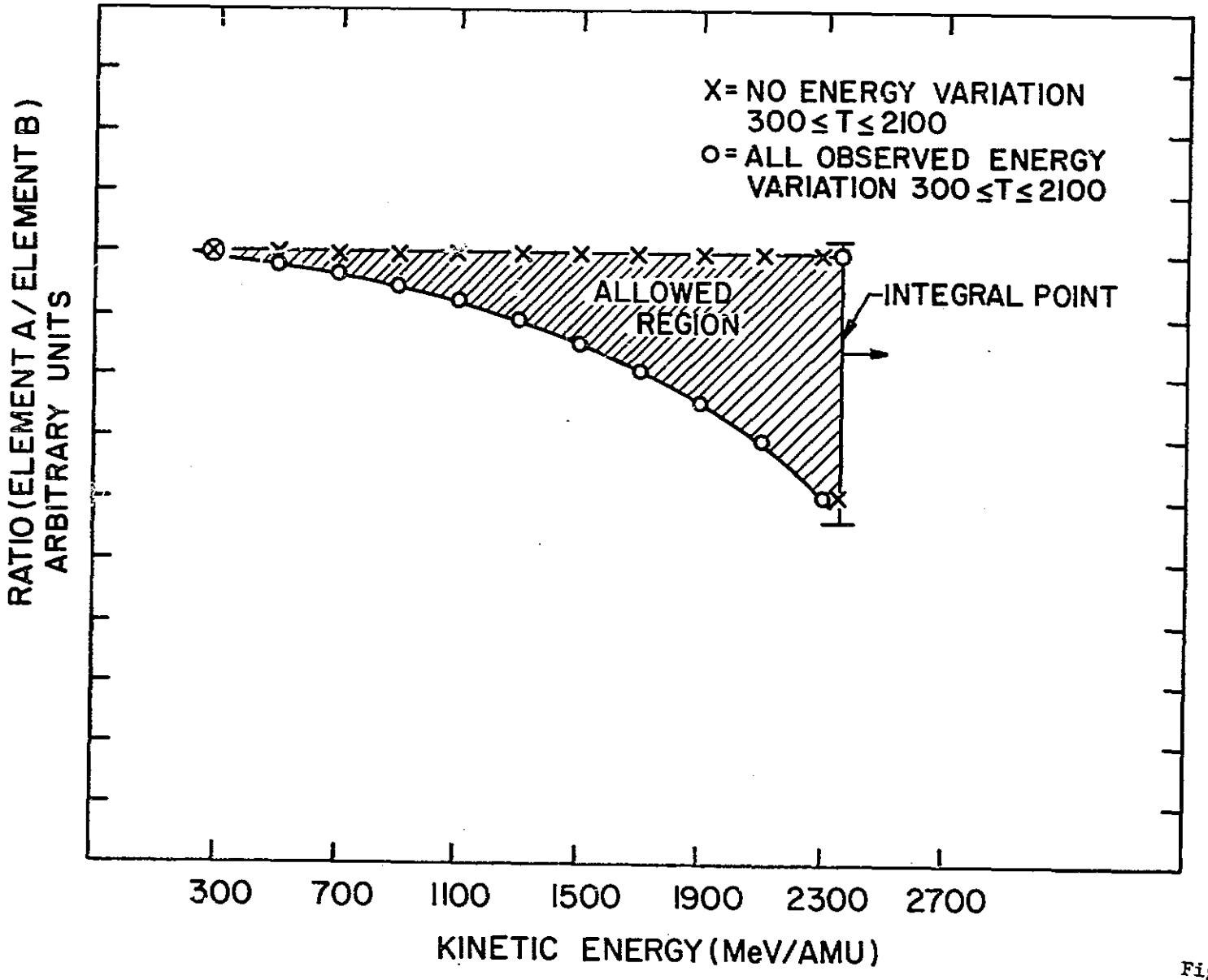

Fig. 6

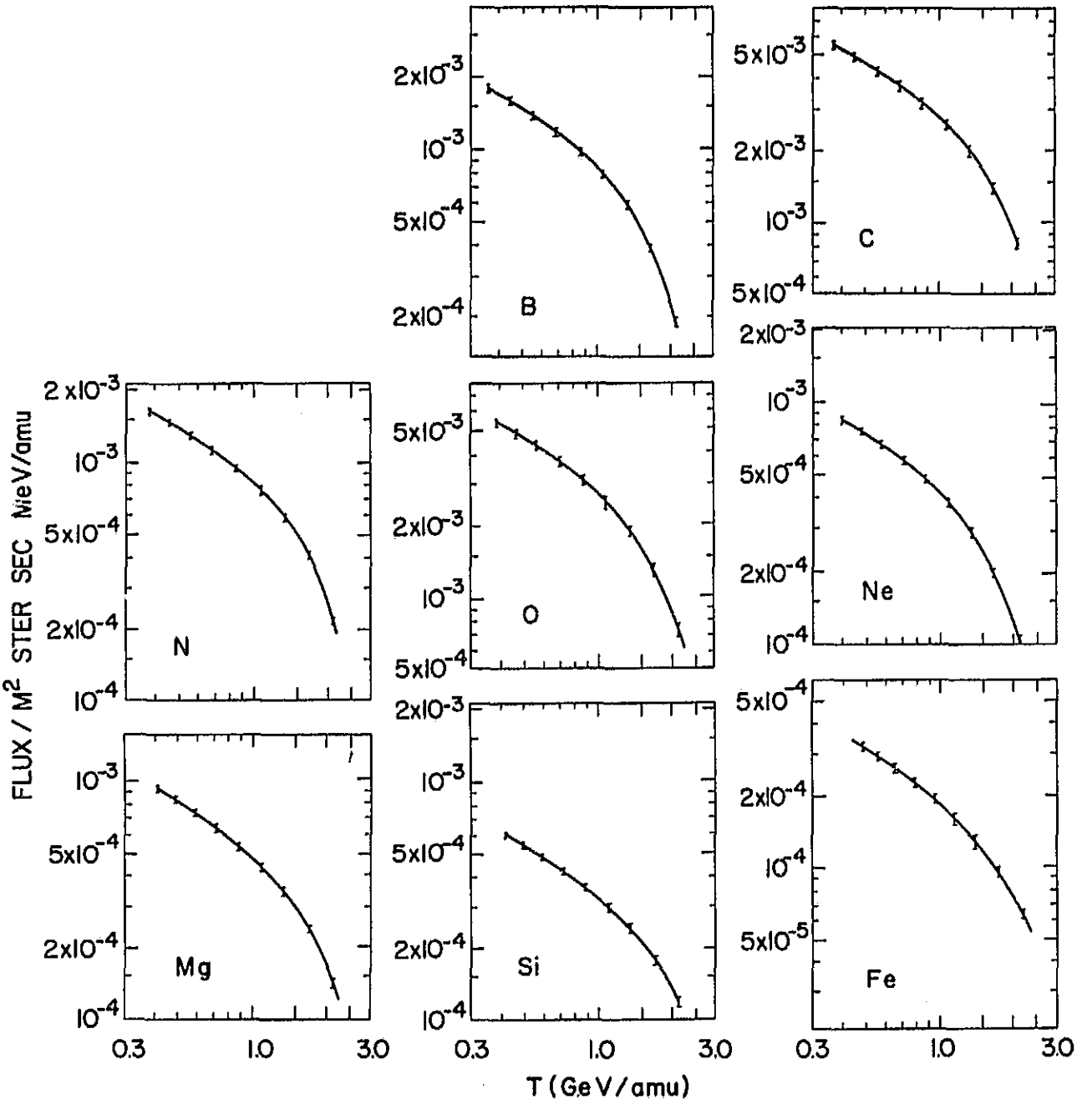

Fig. 7

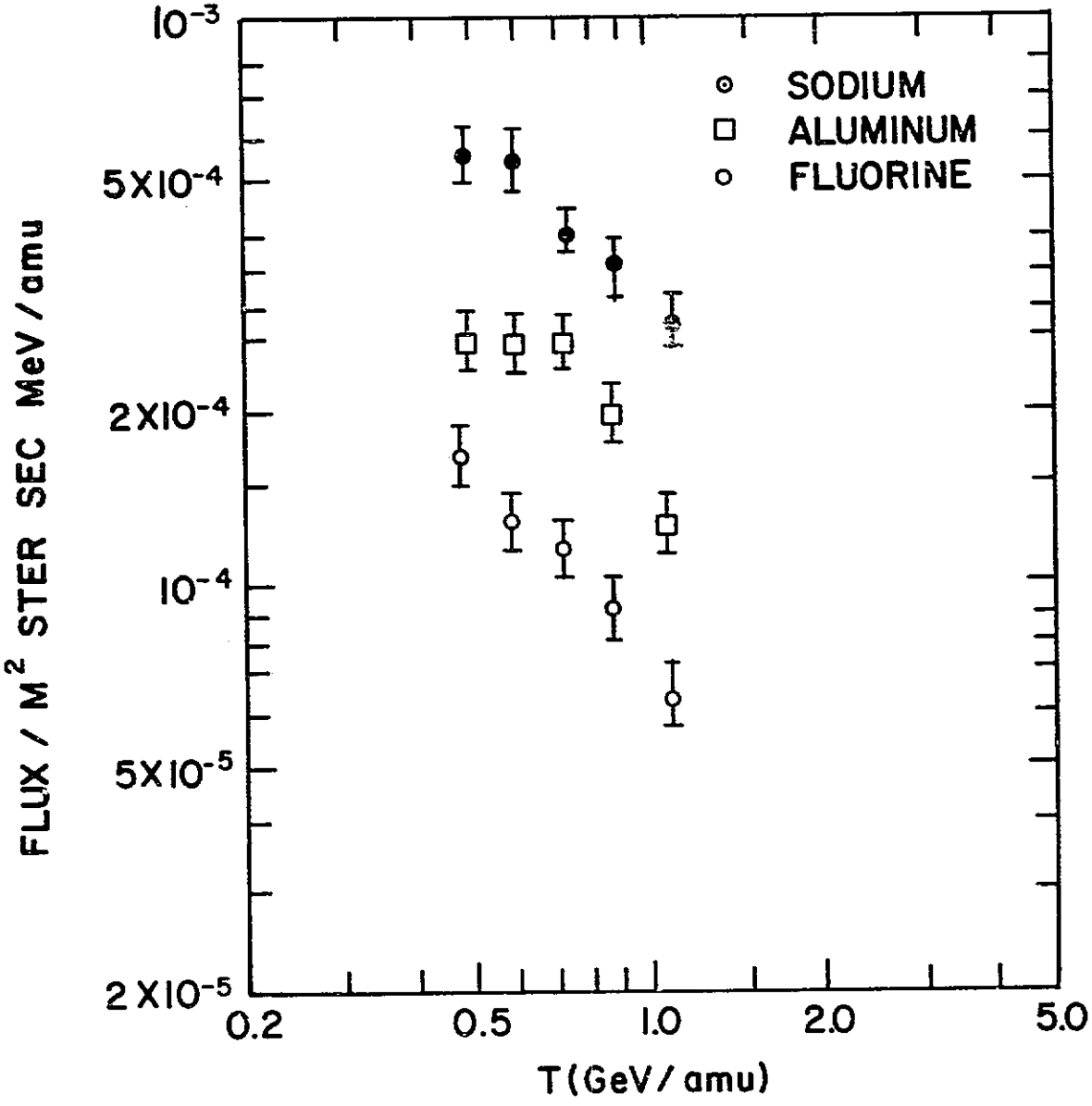

Fig. 8

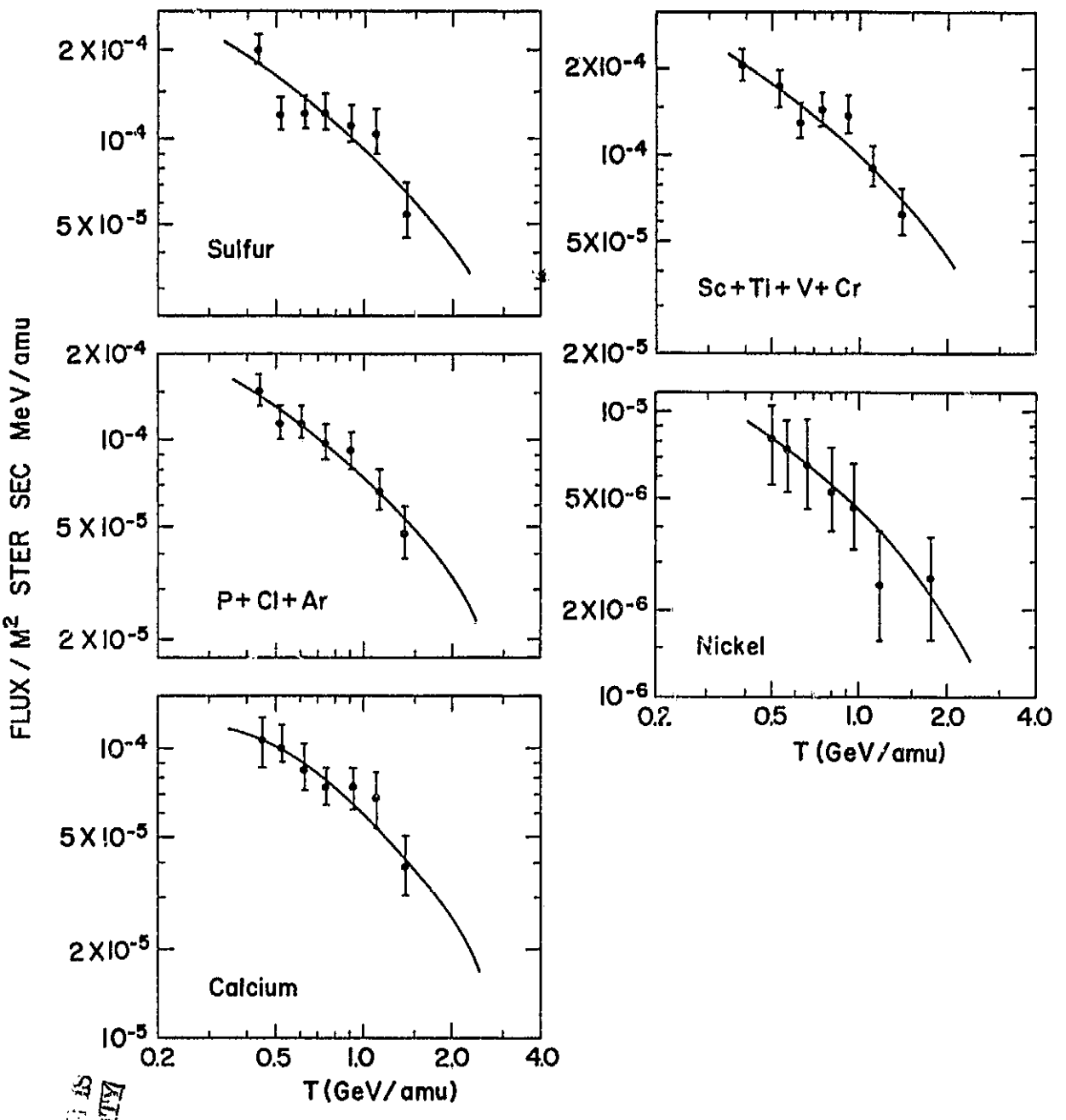
FLUX / M² STER SEC MeV/amu
Sulfur
P+Cl+Ar
Calcium
Sc+Ti+V+Cr
Nickel
T (GeV/amu)
T (GeV/amu)

Fig. 9

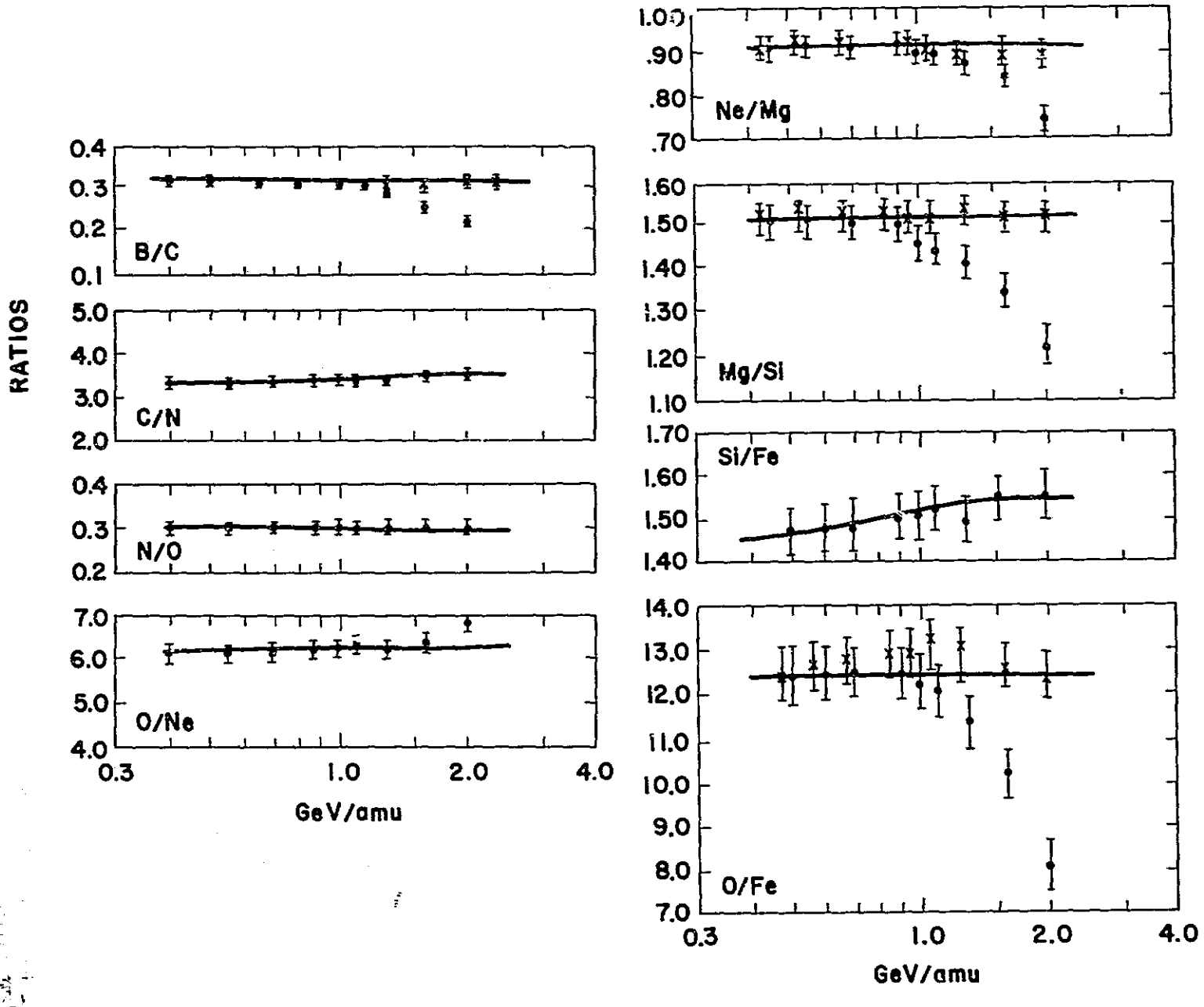

Fig. 10

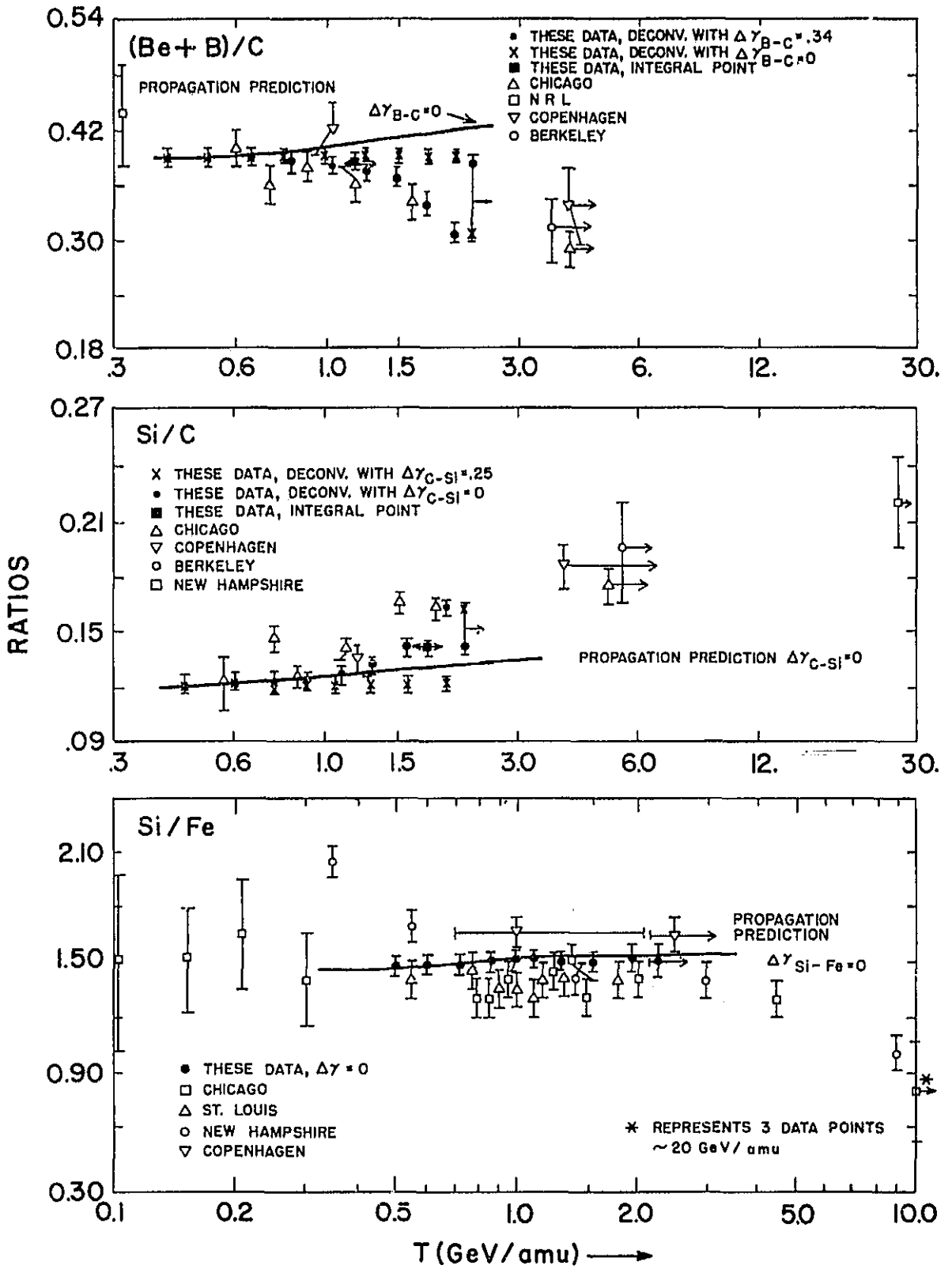
(Be+ B)/C
PROPAGATION PREDICTION
$\Delta\gamma_{B-C}=0$
• THESE DATA, DECONV. WITH $\Delta\gamma_{B-C}=.34$
X THESE DATA, DECONV. WITH $\Delta\gamma_{B-C}=0$
■ THESE DATA, INTEGRAL POINT
△ CHICAGO
□ N R L
▽ COPENHAGEN
○ BERKELEY
0.54
0.42
0.30
0.18
.3
0.6
1.0
1.5
3.0
6.
12.
30.
Si / C
X THESE DATA, DECONV. WITH $\Delta\gamma_{C-Si}=.25$
• THESE DATA, DECONV. WITH $\Delta\gamma_{C-Si}=0$
■ THESE DATA, INTEGRAL POINT
△ CHICAGO
▽ COPENHAGEN
○ BERKELEY
□ NEW HAMPSHIRE
PROPAGATION PREDICTION $\Delta\gamma_{C-Si}=0$
RATIOS
0.27
0.21
0.15
.09
.3
0.6
1.0
1.5
3.0
6.0
12.
30.
Si / Fe
PROPAGATION PREDICTION
$\Delta\gamma_{Si-Fe}=0$
• THESE DATA, $\Delta\gamma=0$
□ CHICAGO
△ ST. LOUIS
○ NEW HAMPSHIRE
▽ COPENHAGEN
* REPRESENTS 3 DATA POINTS ~20 GeV/amu
2.10
1.50
0.90
0.30
0.1
0.2
0.5
1.0
2.0
5.0
10.0
T (GeV/amu) ⟶

Fig. 11

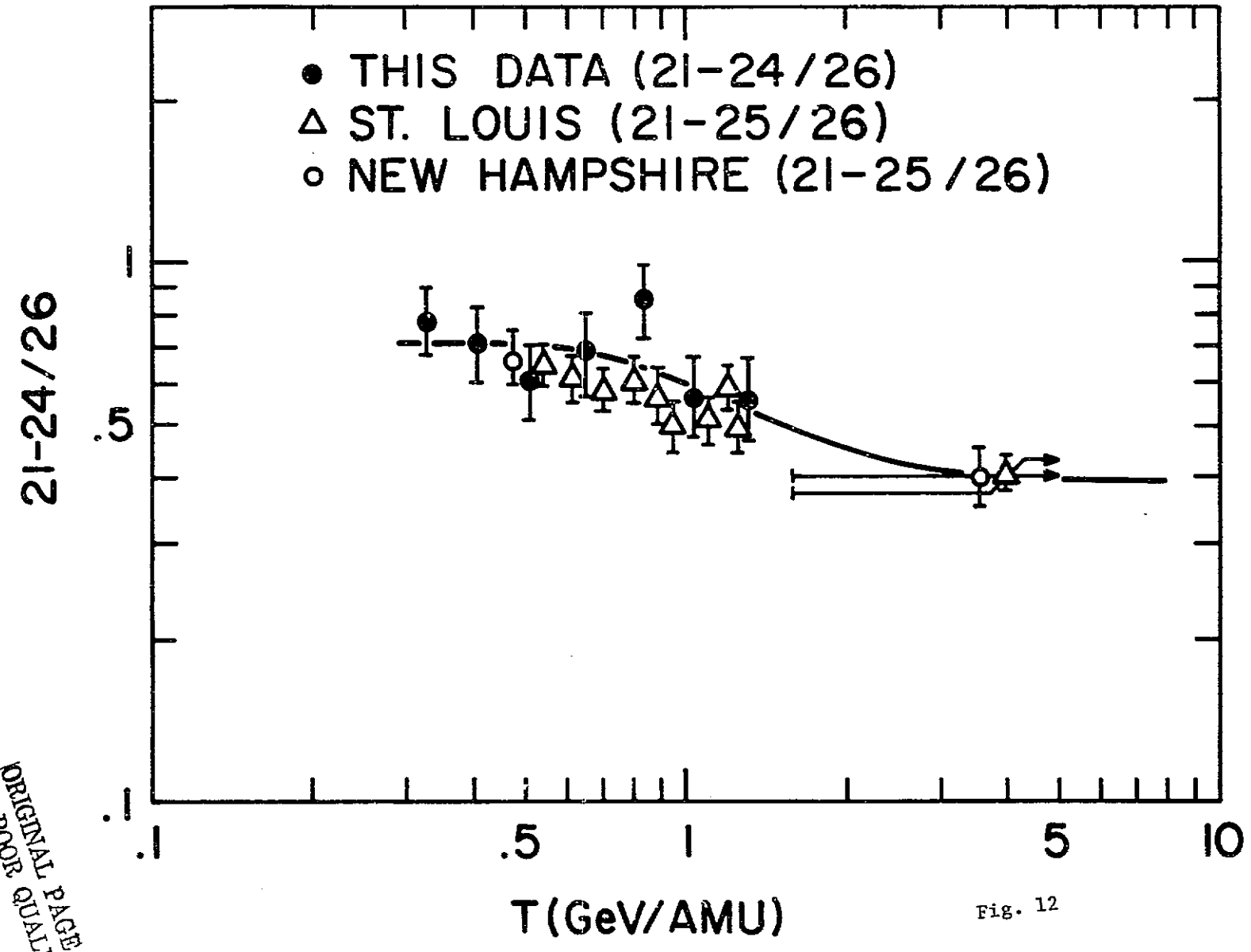

Fig. 12